Development of Cloud Products toward Next Generation Geostationary Meteorological Satellites "Himawari-8/9"

JMA

JMA's mascot character "HARERUN"

Masahiro Hayashi*

*The Meteorological Satellite Center of the Japan Meteorological Agency

masa_hayashi@met.kishou.go.jp

Introduction

The Japan Meteorological Agency (JMA) successfully launched the next-generational satellite "Himawari-8" on Oct. 7th 2014 and plans to commence its operation in 2015 (Figure 1). The Advanced Himawari Imager (AHI) on board Himawari-8/-9 has 16 bands from visible to infrared range (3 visible, 3 near infrared and 10 infrared bands). For the maximum utilization of AHI, JMA has been working on implementation of the *Optimal Cloud Analysis (OCA)* developed by EUMETSAT (EUMETSAT 2011) with EUMETSAT kind cooperation.

OCA adapts the optimal estimation method to retrieve cloud parameters (e.g. cloud optical thickness, cloud effective radius, cloud top pressure and surface temperature). Since different AHI bands have different sensitivity to the parameters as water vapor channels of AHI (band 8-10) has different sensitivity to troposphere heights, high-qualified cloud parameters are expected by applying the optimal estimation method to the multiband data with AHI. In addition to the increased bands, temporal resolution of observation will be enhanced on Himawari-8/9. Cloud parameter retrieval with high-frequency imageries will provide additional information on evolution of cloud systems.

JMA plans to utilize cloud top heights derived from OCA which can treat 2-layer clouds (Watts et al. 2011) to Atmospheric Motion Vector products (AMVs). Multi-layer clouds that are common on the application to the satellite remote sensing make AMVs height assignment (HA) accuracy degraded. Optimal utilization of multi-layered cloud top height to AMV HA algorithm is under investigation at JMA.

Himawari-8/-9 Imager bands (AHI)

Wavelength (μm)	Himawari-8/9		MTSAT-1R/2		GOES-R		MSG	MTG
0.47	●	1			●	1		●
0.51	●	1						●
0.64	●	0.5	●	1	●	0.5	●	●
0.86	●	1			●	1	●	●
0.96								●
1.3					●	2		●
1.6	●				●	1	●	●
2.3	●				●			●
3.9	●		●		●		●	●
6.2	●		●		●		●	●
7	●	2		4	●			●
7.3	●				●		●	●
8.6	●				●	2	●	●
9.6	●				●		●	●
10.4	●		●		●		●	●
11.2	●				●			
12.4	●		●		●		●	●
13.3	●	km		km	●	km	●	●

A sequence of AHI observation in 10 minutes time frame

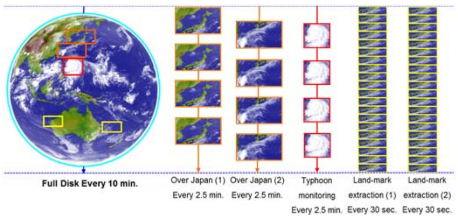

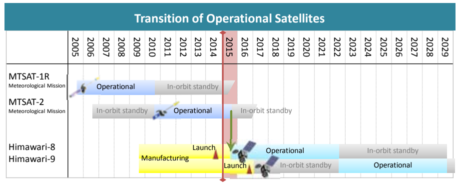

Fig. 1 Schedule and Specification of Himawari-8/9

Algorithm of the Cloud Product (OCA)

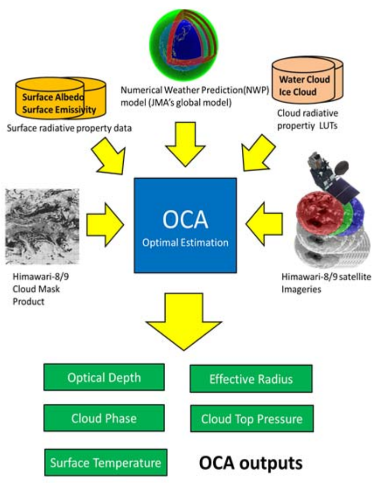

Fig.2 OCA data flow for Himawari-8/9

OCA estimates cloud physical properties ($\boldsymbol{x}$) with multi-channel radiances $\boldsymbol{y}_m$ (from visible to infrared wavelength) by the 1D-VAR method.

In this method, following cost function will be minimized:

$$J = (\boldsymbol{y}_m - f(\boldsymbol{x}))^T S_y^{-1} (\boldsymbol{y}_m - f(\boldsymbol{x})) + (\boldsymbol{x} - \boldsymbol{x}_a)^T S_x^{-1} (\boldsymbol{x} - \boldsymbol{x}_a)$$

The cost function is minimized by the Levenburg-Marquardt Descent

$$\delta \boldsymbol{x} = -\left(\frac{\partial^2 J}{\partial \boldsymbol{x}^2} + \alpha \boldsymbol{I}\right)^{-1} \frac{\partial J}{\partial \boldsymbol{x}}$$

S: error covariance matrix
$\boldsymbol{x}_a$: a priori state vector
α: Marquardt parameter

The forward model $f(\boldsymbol{x})$ is divided by two wavelength range :

Short Wave Radiation (visible to near-infrared)

$$f(\boldsymbol{x}) = T_{2ac}\rho_{BD} + \frac{T_{2ac} T_B T_D \rho_S}{1 - T_{2bc}\rho_D \rho_S}$$

Clear sky atmospheric transmission (T_{2ac}, T_{2bc})
→ fast radiative calculation with NWP model (RTTOV11 Hocking et al. 2013)
Cloud reflection (ρ_{BD}, ρ_D) and transmission (T_B, T_D)
→pre-calculated LUT (DISORT Stemnes et al. 1988)
Surface BRDF (ρ_S)
→Land: climatology (MODIS White Sky Albedo Moody et al. 2005), Sea: Cox & Munk 1954

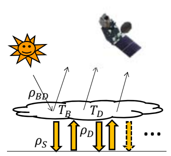

Long Wave Radiation (infrared)

$$f(\boldsymbol{x}) = R_{bc} T_D T_{ac} + B(T)\varepsilon_c T_{ac} + R_{ac}^{\downarrow} \rho_D T_{ac} + R_{ac}$$

Clear sky atmospheric transmission (T_{ac}, T_{bc}) and radiation ($R_{ac}, R_{ac}^{\downarrow}$)
→ fast radiative calculation with NWP model (RTTOV11)
Cloud reflection (ρ_D), emissivity (ε_c) and transmission (T_D))
→pre-calculated LUT (DISORT)
Radiance below the cloud (R_{bc})
→NWP model, OCA parameter (surface temperature) and surface emissivity (Land: climatology Seemann et al. 2008, Sea : Masuda 2006)

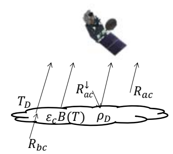

Cloud Properties

- Water cloud

Water clouds are assumed to aggregation of spherical droplets and the scattering properties are computed with the Lorenz-Mie theory of scattering. The log-normal size distributions (Hansen and Travis 1974) are used for the LUT calculation

- Ice cloud

To prepare non-spherical ice scattering properties for AHI bands, the Meteorological Research Institute (MRI) of JMA has computed single-scattering radiative properties with the methods of FDTD , improved geometric optics (GOM2) and geometric optics (GOM) (Ishimoto et al. 2012) for AHI spectral response functions. Currently the solid column and Voronoi aggregate are availabe (Upper of Figure 3). The modified gamma functions are adapted for the ice cloud size distributions. Figure 3 shows an example of the non-spherical ice cloud scattering property (phase function) used for the LUT computation

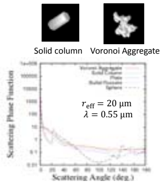

Fig. 3 Size-averaged phase functions of various ice habits

Preparation for Himawari-8/9

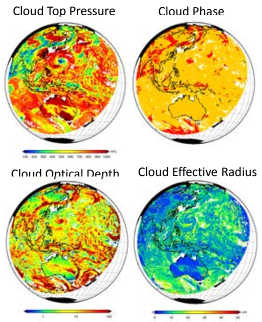

Fig. 5 An Example of OCA outputs from Simulated Himawari-8 imageries (Jul. 10th 2014 04 UTC) Only the daytime pixels are shown

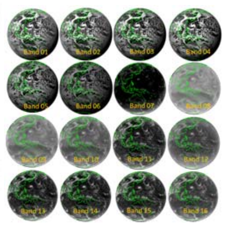

Fig. 4 Simulated AHI images (Jul. 10th 2014 04 UTC)
Reflectivity: Band01-06
Brightness Temperature : Band07-16

JMA has implemented the OCA and investigated it with SEVIRI data (Hayashi 2014). Besides the real data as proxy of AHI data, simulated Himawari-8 imageries from JMA's global model via radiative transfer model (RSTAR; Nakajima and Tanaka 1986) are created for the purpose of the products test operation at MSC (please see http://www.data.jma.go.jp/mscweb/en/himawari89/space_segment/spsg_ahi_proxy.html for the details of simulated imageries). Figure 4 shows an example of the 16-bands Himawari-8 simulated imageries at July 10th 2014 04 UTC.

Figure 5 is an example of the OCA outputs used the imageries of Figure 4. While cloud optical depths, cloud phase and cloud top pressures are derived naturally, derived effective radiuses seems to be unnatural compared to the case of real data, as ice cloud water's effective radius over the ocean is quite small and and water clouds edge pixels have relatively high effective radius. As for the former case, it is because that simulated near-infrared bands (band 05 and band 06) have relatively high reflectivity on the ice clouds. One possible reason is considered that JMA's global NWP model does not have enough cloud microphysical value and used empirical methods (similar to Slingo 1989) to estimate effective radius for inputting the RSTAR simulations. The latter case of high cloud effective radius could be from poor cloud masking that discriminates "actually" clear-sky pixels as cloudy pixels.

Future plans

Currently Himawari-8 is in 100-day Running Test (Figure 6) and preparation of its operation is going well. The first images of Himawari-8 are shown Figure 7. Investigations of the OCA derived from the real images of Himawari-8 is being conducted at JMA. After the validation of OCA used the real data, the two-layer mode of OCA (Watts et al. 2011) will be implemented.

Related to the previous section, analysis of simulated AHI imageries from cloud resolving high resolution NWP model will be planned for the error analysis.

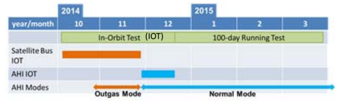

Fig. 6 Detailed Schedule of Himawari-8

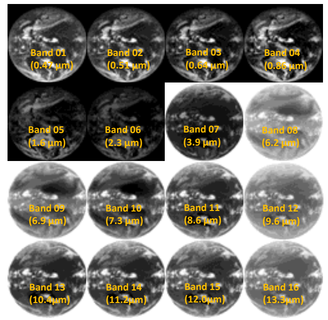

Fig. 7 Himawari-8 first imageries (Dec. 18 2014 02:30 UTC)

Acknowledgement

This work is greatly supported by EUMETSAT. I am really grateful to Phil Watts for kind advices and providing many materials of OCA. I thank to MRI/JMA for providing sea surface emissivity calculation code and scattering database for this work. This research was supported in part by JST, CREST.

Reference

Cox C. and W. Munk, 1954: Measurement of the Roughness of the Sea Surface from Photographs of the Sun's Glitter. *J. Opt. Soc. Am.* **44**, 838-850

EUMETSAT, 2011: ATBD for Optimal Cloud Analysis Product. EUMETSAT

Ishimoto H., K. Masuda, Y. Mano, N. Orikasa and A. Uchiyama, 2012: Irregularly Shaped Ice Aggregates in Optical Modeling of Convectively Generated Ice Clouds. *JQSRT*, **113**, 632-643

Hayashi M., 2014 : Introduction of the Optimal Cloud Analysis for Himawari-8/-9, *Cloud Retrieval Evaluation Workshop-4, Germany*

Hocking, J, P. Rayer, D. Rundle, R. Saunders, M. Matricardi, A. Geer, P. Brunel and J. Vidot, 2013: RTTOV v11 Users Guide. *NWP SAF*

Moody E.G., M. D. King, S. Platnick, C. B. Schaaf and F. Gao 2005: Spatially Complete Global Spectral Surface Albedos: Value-Added Datasets Derived. *IEEE Trans. Geo. And Rem. Sen.*, **43**, 144-158

Masuda K., 2006: Infrared sea surface emissivity including multiple reflection effect for isotropic Gaussian slope distribution model, *Rem. Sen. Env.*, **103**, 488-496

Nakajima, T. and M. Tanaka, 1986: Matrix formulation for the transfer of solar radiation in a plane-parallel scattering atmosphere. *J. Quant. Spectrosc. Radiat. Transfer*, **35**, 13-21.

Seemann W. S., E. E. Borbas, R. O. Knuteson, G. R. Stephenson and H.-L. Huang, 2008: Development of a Global Infrared Land Surface Emissivity Database. *J. Appl. Meteor.*, **47**, 108-123

Slingo A., 1989: A GCM parameterization for the shortwave radiative properties of water clouds, *J. Atmos. Sci.*, **46**, 1419-1427

Stemnes K., S.-C. Tsay, W Wiscombe and K. Jayaweera, 1988: Numerically Stable Algorithm for Discrete-Ordinate-Method Radiative Transfer in Multiple Scattering and Emitting Layered Media, *App. Opt*, **27**, 2502-2509

Watts P. D., C. T. Mutlow, A. J. Baran, and A. M. Zavody 1998: Study on Cloud Properties Derived from Meteosat Second Generation Observation. *EUMETSAT*

Watts P. D., R. Bennartz and F. Fell, 2011: Retrieval of Two-layer Properties from Multispectral Observations Using Optimal Estimation. *J. Geophys. Res.*, **116**, D16203